The effect of block lengths on micelle structure in blends of styrene–isoprene diblock copolymer and poly(vinyl methyl ether)

Jong-Hyun Ahn, Byeong-Hyeok Sohn, Wang-Cheol Zin[*]

Department of Materials Science and Engineering and Polymer Research Institute, Pohang University of Science and Technology, Pohang 790-784, South Korea

Abstract

The micellar structure of styrene–isoprene diblock copolymer and poly(vinyl methyl ether) blends was investigated by using small-angle X-ray scattering and transmission electron microscopy techniques. In order to determine the effect of styrene block length on the formation of micellar structure, three sets of diblock copolymers, with near-identical isoprene block molecular weights, but with different styrene block lengths were studied. With modeling based on the polydisperse Percus–Yevick hard sphere fluid model, the structural parameters characterizing the micelles were determined as a function of copolymer concentrations, temperature, and copolymer block lengths. The core radius was found to decrease on increasing the length of styrene block. The degree of swelling of the corona by PVME increased steadily with increasing the styrene block length. © 2002 Elsevier Science Ltd. All rights reserved.

Keywords: Micelle; Block copolymer; Blend

1. Introduction

Blends of a block copolymer and a homopolymer form a variety of morphologies such as lamellar, cylindrical, bicontinuous gyroid, and spherical [1–4]. When the AB diblock copolymer is mixed with a large amount of homopolymer which is miscible with one component of the blocks, the mixture may form a spherical micellar phase. The spherical micelles are made up of two regions: the core, composed of almost pure B blocks, and the corona, which contains the A blocks of the copolymer swollen by homopolymer chains.

Considerable theoretical and experimental works have reported on the micellar behavior of AB/A blends [5–15]. Rigby and Roe have studied the formation of spherical micelle in blends of styrene–butadiene diblock copolymer (SB) and low molecular weight polybutadiene by varying temperature, copolymer concentration, and relative block lengths [5,6]. Kinning et al. have also investigated the effect of styrene, butadiene block molecular weights, and polystyrene (PS) homopolymer molecular weights on the micelle structure of SB and PS blends [9,10]. However, all the above investigations were concerned with AB/A blends. Only a few studies have dealt with the micelle formation in blends of an AB diblock copolymer with a third C polymer that is miscible with one block but immiscible with the other [16].

In a previous work [17], we reported the micelle formation and the phase behavior of styrene–isoprene diblock copolymer (SI) and poly(vinyl methyl ether)(PVME) blend exhibiting a lower critical solution temperature. These micelles consist of a spherical isoprene block core surrounded by a corona containing styrene blocks swollen with PVME. With all concentrations, the core radius remains fairly constant up to the macrophase separation temperature. In the present work, we investigated the effect of styrene block length on the micellar structure of SI/PVME blends. For this purpose, two more blend systems containing PVME and SI diblock copolymers have been studied. SI diblock copolymers have the molecular weight of isoprene blocks kept in a relatively constant state and that of the styrene block varied.

2. Experimental

2.1. Materials

The characteristics of the polymers used are listed in Table 1. Three SI diblock copolymers were synthesized by living anionic polymerization. Neat SI1510, SI2510, and SI4510 have lamellar, cylindrical and spherical

* Corresponding author. Tel.: +82-54-279-2136; fax: +82-54-279-2399.
E-mail address: wczin@postech.ac.kr (W.-C. Zin).

Table 1
The characteristics of the polymers used

Sample code	M_w[a]	M_w of styrene block[b]	M_w of isoprene block[b]	M_w/M_n[c]	Styrene content[b] (wt%)
SI4510	51 200	41 900	9300	1.05	82
SI2510[d]	35 000	25 200	9800	1.02	72
SI1510	22 500	13 500	9000	1.05	60
PVME	81 000	–	–	1.69	–

[a] By low-angle laser light scattering.
[b] By ^{1}H-NMR.
[c] By GPC calibrated with PS standard.
[d] The same material used in Ref. [17].

microdomain morphologies, respectively. PVME was a commercially available material (Aldrich Co.), which was dissolved by toluene, purified by activated carbon powder, and precipitated twice by a large amount of *n*-hexane. Blends with various fractions were prepared by casting from toluene solution in presence of antioxidant (Irganox 1010, Ciba-Geigy Group) and then slowly evaporating the solvent for 5 days. The samples were then dried under a vacuum at room temperature over a period of 1 week.

2.2. Small-angle X-ray scattering

Small angle X-ray scattering (SAXS) measurements were performed with point focusing at 4C1 beamline using synchrotron X-ray radiation sources at Pohang Accelerator Laboratory, Korea. The X-ray wavelength used was 1.608 Å. A one-dimensional position sensitive detector (Model 1412XR, EG&G Princeton Applied Research) was employed with an interface system (Model 1463, EG&G). The distance between the sample and detector was 1.5 m. The samples were held in an aluminum holder which was sealed with two pieces of 8 μm Kapton film after which the aluminum holder was inserted into a brass frame fastened by screws to prevent the sample from leaking out of the aluminum holder upon subsequent heating and cooling. Such samples had a thickness of about 1 mm, and were heated up to 180 °C at the rate of 2 °C/min while the intensity data was being collected through the detector and computer interface every 2.5 min for 1 min. The measured SAXS intensity was corrected for the decrease of the ring current, background scattering, and absorption by sample. The correction for smearing effect by the finite cross section of the incident beam was not necessary for the optics of SAXS with point focusing. The data are presented as a function of $q = 4\pi(\sin\theta)/\lambda$, where 2θ and λ are scattering angle and X-ray wavelength, respectively.

The following specific volume values were used to calculate the electron density at various temperatures [6,18]

$$V_{PS}(PS) = 0.9369 + 2.006 \times 10^{-4}T + 2.470$$

$$\times 10^{-7}T^2 \text{ (below } T_g),$$

$$V_{PI}(PI) = 1.0771 + 7.22 \times 10^{-4}T + 2.46 \times 10^{-7}T^2,$$

$$V_{PVME}(PVME) = 1/(1.0725 - 7.259 \times 10^{-4}T + 1.160$$

$$\times 10^{-7}T^2)$$

where T denotes the temperature in degrees centigrade.

2.3. Transmisson electron microscopy

The samples were prepared by placing a drop of solution on a carbon-/formvar-coated copper grid and letting the solvent evaporate at room temperature. To remove the substrate and the solvent evaporation effects that may affect the observed morphology of solution cast block copolymer, the solvent was very slowly evaporated and the samples were annealed at 35 °C for a day to attain equilibrium morphology. Then, the samples were exposed to the vapor of a 2% aqueous OsO_4 solution. OsO_4 is a selective staining agent for the isoprene blocks. Because of selective staining, isoprene domains appear black and the PVME matrix white in TEM micrographs. TEM was performed on a JEOL 1200EX electron microscope operated at 120 kV.

Although TEM image of bulk samples is necessary in order to obtain more detailed observation, the solvent cast process on a grid was used since cryoultra-thin section of bulk samples was very difficult. However, in previous work there was not much difference between TEM results from bulk samples and those from solvent cast process [17].

2.4. Data analysis of SAXS measurements

The model that has been used for analyzing the SAXS data is based on the assumption of a micelle with the core of the dense isoprene-block chains, surrounded by the corona of styrene-block chains swollen with PVME. Since the electron density of PVME ($\rho = 349$ e/nm^3 at room temperature) is almost equal to that of PS ($\rho = 340$ e/nm^3), it can be considered that PVME matrix has the same electron density as the corona region.

The monodisperse intensity for a monodisperse system of micelles can be written as

$$I(q) = (\Delta\rho)^2 N|F(q)|^2 S(q) \tag{1}$$

where $(\Delta\rho)^2$ is the contrast factor, N the number density of the micelles, $F(q)$ the single particle form factor, and $S(q)$ is the interparticle structure factor.

For a homogeneous sphere of radius R, the form factor is defined by

$$F(q) = \frac{4\pi}{q^3}[\sin(qR) - qR\cos(qR)] \qquad (2)$$

Using the classical Ornstein–Zernike approximation for the spatial correlation fluctuations and the Percus–Yevick (PY) approximation for hard-sphere fluids, the structure factor is given by [19,20]

$$S(q) = \frac{1}{1 + 24\eta G(2qR_{HS}, \eta)/(2qR_{HS})} \qquad (3)$$

where G is a trigonometric function of R_{HS} and η is the hard sphere volume fraction ($\eta = 4\pi N R_{HS}^3/3$).

For these micellar systems, there will inevitably be some distribution in the size of the micelle core and the corona region. To observe the effects of polydispersity of particles, Eq. (1) is rewritten by [6,21]

$$I(q) = (\Delta\rho)^2 N\langle|F(q)|^2\rangle S'(q) \qquad (4)$$

where $S'(q)$ acts as an apparent structure factor. By assuming that particle size and position are uncorrelated, it is defined by

$$S'(q) = 1 + \beta(q)[S(q) - 1] \qquad (5)$$

where

$$\beta(q) = |\langle F(q)\rangle|^2/\langle|F(q)|^2\rangle \qquad (6)$$

To evaluate the average of the form factor $F(q)$, we assume the micelle core radii to be distributed according to the Flory–Schultz distribution

$$W(R) = (1/Z!)b^{Z+1}R^Z\exp(-bR) \qquad (7)$$

where the parameter Z characterizes the width of the distribution ($Z = \infty$ corresponding to a δ function) and parameter b is related to the number-average radius $\langle R\rangle$ by $b = (Z+1)/\langle R\rangle$. The root mean square deviation from the mean is given by $\sigma_R = (\langle R^2\rangle - \langle R\rangle^2)^{1/2} = \langle R\rangle/(Z+1)^{1/2}$.

Thus, the scattered curves can be fitted using a least-squares routine to Eq. (4), yielding the four parameters; Z, $N(\Delta\rho)^2$, $\langle R_c\rangle$, and $\langle R_{HS}\rangle$.

3. Results and discussion

Fig. 1(a) shows the results of SAXS measurements on SI4510/PVME blends with various concentrations at room temperature. At the lowest copolymer concentration, intensity decreases monotonically by increasing the scattering vector, q, which exhibits a characteristic of micellar scattering. With blends containing larger amounts of copolymer,

the intensity curves show a maximum due to the contribution of interparticle interference. An electron micrograph of a blend containing 7 wt% copolymer confirms that the spherical micelles are randomly dispersed, as shown in Fig. 1(b).

The miscibility of the SI4510/PVME blend at room temperature is driven by negative interaction energy density ($\Lambda_{SB/PVME}$) between styrene blocks and PVME. However, the SI4510/PVME blend undergoes a macrophase separation by the reduction of attractive interaction upon raising temperature. Fig. 2 shows the SAXS profiles for blends containing 7 wt% copolymer in the temperature range from 30 to 100 °C. The scattered intensity which arose isolated micelle gradually decreases in magnitude as the temperature is raised. Above 60 °C, however, the peak which arose from the interdomain of block copolymer begins to appear at the low-q position, signaling the macrophase separation between SI4510 and PVME. Therefore, the
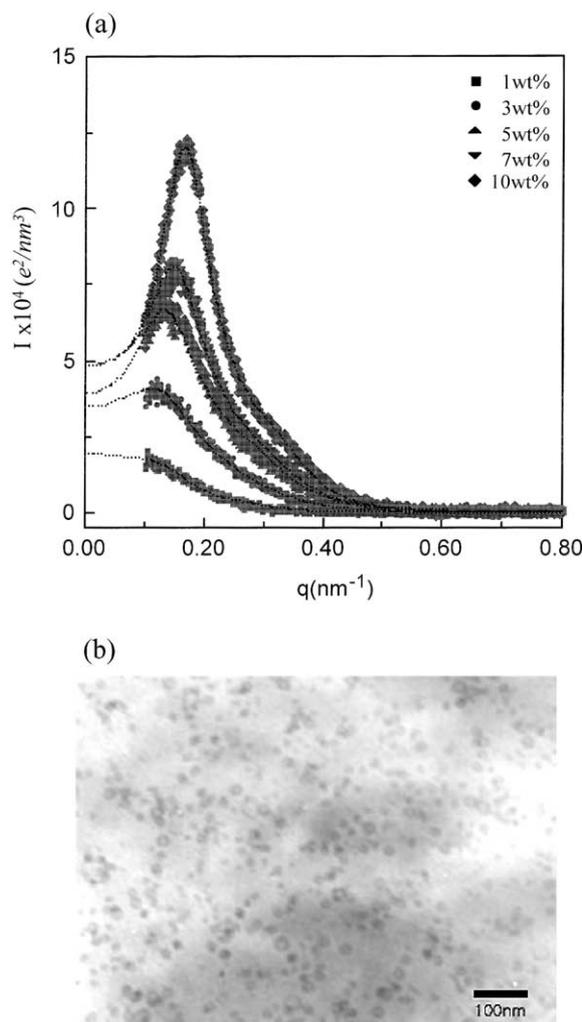

Fig. 1. (a) Scattered X-ray intensity obtained from SI4510/PVME blends at various copolymer concentrations. The dotted line indicates the best fit to the SAXS patterns obtained with the PY hard-sphere liquid model. (b) TEM image for SI4510/PVME blend containing 7 wt% copolymer. The scale bar denotes 100 nm.
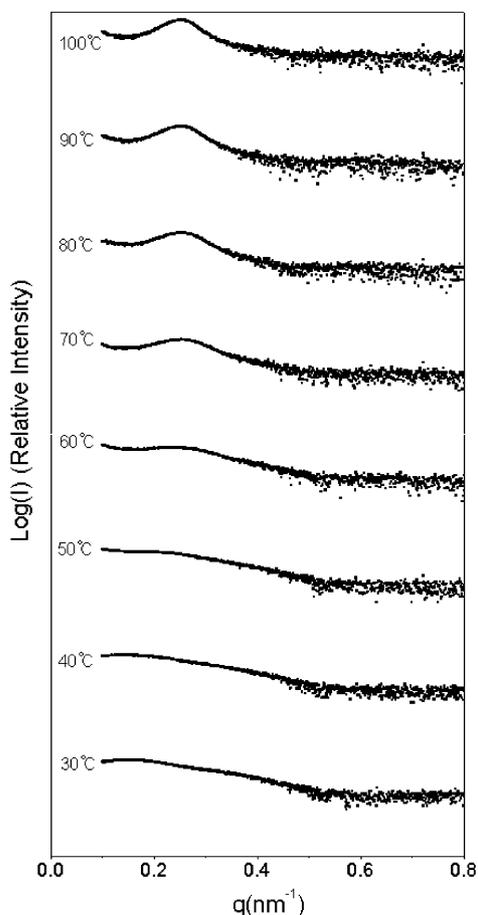
Fig. 2. Temperature dependence of SAXS profiles for the SI4510/PVME blend containing 7 wt% copolymer.

micelle structure of the SI4510/PVME blend can only be determined below macrophase separation temperature.

Fig. 3(a) shows the SAXS patterns for the SI1510/PVME blend. For blends containing 1, 3 and 5 wt% SI1510, the SAXS patterns exhibit a micellar scattering as seen in SI4510/PVME blend. However, the patterns for the blends of 7 and 10 wt% copolymer concentration do not show a low-angle interparticle interference maximum in contrast to those of the SI4510/PVME and SI2510/PVME blend [17]. The electron micrographs in Fig. 3(b) and (c) show that the blend containing 3 wt% copolymer forms spherical micelles and the blend containing 7 wt% copolymer forms both spherical micelles of large size and a macroscopically phase-separated structure similar to the onion-like domains observed in blends of SI and PS homopolymer [22]. This macrophase-separated structure appears to consist of SI1510-rich macrodomains dispersed in the PVME-rich matrix. The macrodomains rich in SI1510 are composed of alternating lamellae of styrene and isoprene micro-domains which correspond to the equilibrium morphology of neat SI1510. The absence of the interlamellar peak in Fig. 3(a) is, however, puzzling.

It is interesting to note that SI1510/PVME blend exhibits a lower macrophase separation temperature than SI4510/
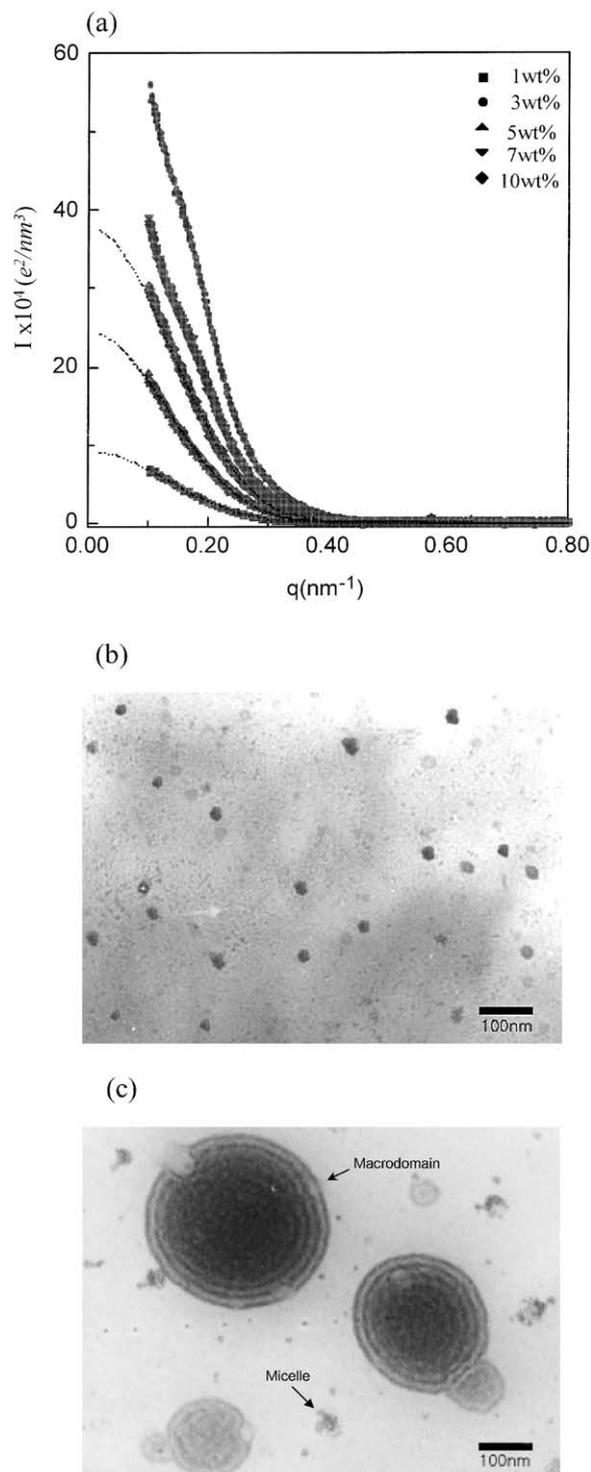

Fig. 3. (a) Scattered X-ray intensity obtained from SI1510/PVME blends at various copolymer concentrations. (b) TEM image for SI1510/PVME blend containing 3 wt% copolymer. (c) TEM image for SI1510/PVME blend containing 7 wt% copolymer. The scale bar denotes 100 nm.

PVME and SI2510/PVME blends. The decrement of the macrophase separation temperature with a decrease in the molecular weight of the styrene block may be understood by considering the change in the conformational entropy of the
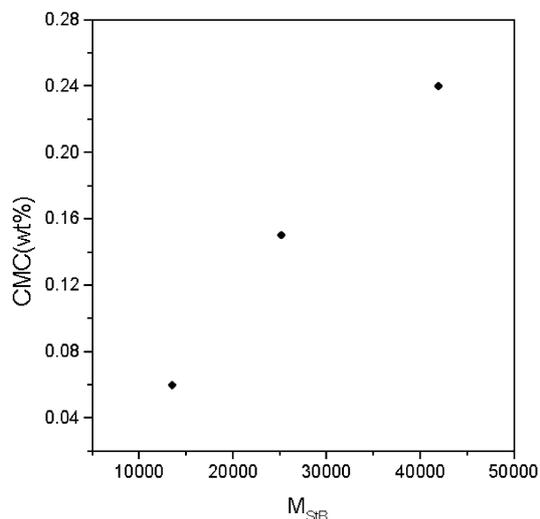
Fig. 4. Effect of styrene block length on cmc.

PVME chains [23,24]. The confinement of the added PVME chains into the styrene microdomain gives rise to a loss in the conformational entropy of the PVME chains, which is unfavorable to mixing of PVME and the styrene blocks. The loss in conformational entropy increases by decreasing the spacing of the styrene micro-domains, and, the solubility of PVME into styrene micro-domain becomes lowered with a decrease in the molecular weight of styrene block. Thus, the macrophase separation temperature is lowered with a decrease in the molecular weight of the styrene block.

The critical micelle concentration (cmc) determined by extrapolating the invariant to zero is shown in Fig. 4 for
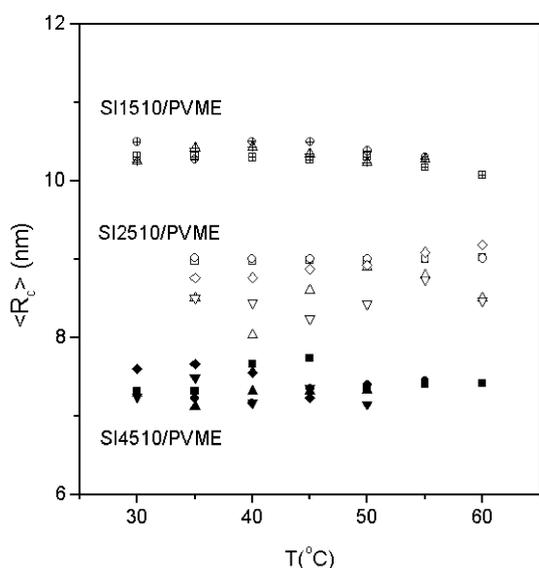

Fig. 5. The core radius, $\langle R_c \rangle$ of spherical micelles is plotted against temperature for the three series of blends containing 1 wt% copolymer (squares), 3 wt% copolymer (circles), 5 wt% copolymer (upward-facing triangles), 7 wt% copolymer (downward-facing triangles) and 10 wt% copolymer (diamonds).

SI4510, SI2510, and SI1510 in PVME. The cmc increases from 0.06 to 0.24 wt% with increasing the molecular weight of styrene blocks. The increment of cmc indicates that the compatibility between the copolymer and homopolymer increases as the proportion of styrene block increases.

The SAXS data are further analyzed by methods appropriate to systems consisting of suspensions of spherical particles. It was well-known that the PY solution for the structure factor of hard-sphere liquids can serve as a model for calculating predicted scattering curves to fit observed data and thereby allow the evaluation of parameters characterizing block copolymer micelles [6,17,21]. With use of the four parameters, Z, $N(\Delta\rho)^2$, the micelle core radius, $\langle R_c \rangle$, and effective hard sphere radius, $\langle R_{HS} \rangle$, the calculated curves were fitted against the observed data by nonlinear least squares fitting procedure as seen in Figs. 1(a) and 3(a). Although it is difficult to determine uniquely four parameters for the SAXS profile exhibiting no peak, the parameters determined by this fitting method had reasonable values with little error, compared with those determined from the SAXS curve of blend exhibiting a peak.

Fig. 5 shows the values of $\langle R_c \rangle$ thus evaluated for the three sets of samples containing copolymer. The core radius remains at a fairly constant value up to about 50 °C (above this temperature, macrophase separation begins to occur by the decrease in miscibility between SI and PVME). For the same copolymer the variation in $\langle R_c \rangle$ upon concentration is very minor. It is also found that for these three blends, the core radius decreases with increasing the styrene block length.

This phenomenon can be understood by the effect of mixing entropy. As the ratio of PVME to styrene block molecular weight, M_{PVME}/M_{StB}, decreases, the mixing entropy of the styrene block chains and homopolymer is increased. The increased mixing entropy gives rise to the change in micelle structure as follows: (1) the volume fraction of PVME in the corona region increases, and thus corona thickness becomes larger, and (2) the micelle core size decreases as a result of fewer copolymer chains per micelle. However, the concentration of PVME, which can be solubilized in the corona region, is somewhat limited because the stretching of styrene block chains in the corona causes a loss of conformational entropy in the styrene chains. Therefore, the thickness of the corona region can be determined by a balance of two opposing factors.

Fig. 6 shows corona thickness values of micelles containing SI4510, SI2510, and SI1510, respectively. The thickness of the corona (L) is then given by

$$L = \langle R_{HS} \rangle - \langle R_c \rangle \qquad (8)$$

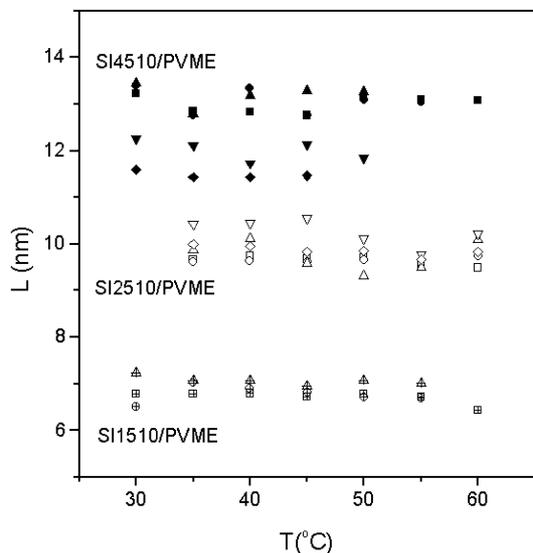As one would expect, the corona thickness increases with an increase in styrene block molecular weight.

Fig. 6. The corona thickness, L of spherical micelles is plotted against temperature for the three series of blends containing 1 wt% copolymer (squares), 3 wt% copolymer (circles), 5 wt% copolymer (upward-facing triangles), 7 wt% copolymer (downward-facing triangles) and 10 wt% copolymer (diamonds).
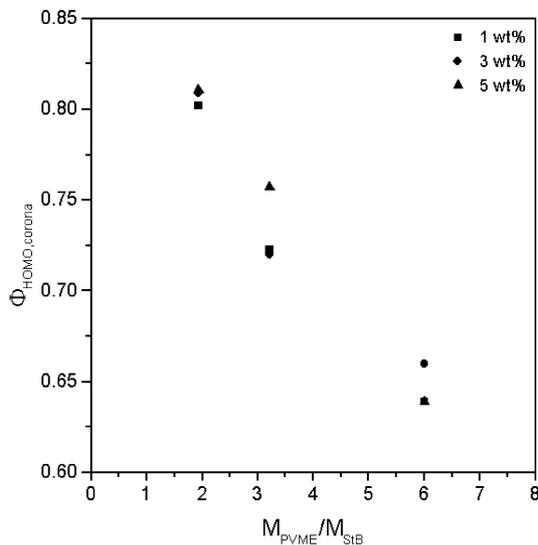

Fig. 7. Volume fraction of PVME in the corona region is plotted against the ratio of the PVME molecular weight to that of styrene block for SI4510, SI2510, and SI1510.

From the earlier results it is worthwhile to note the volume fraction of the homopolymer that is present within the micelle corona of blends. With the assumption that the micelle core consists of only the isoprene blocks, the number of block copolymer molecules per micelle (p) can be estimated by the following equation:

$$p = \frac{4}{3}\pi R_c^3 / v_{PI} \tag{9}$$

where v_{PI} denotes the molecular volume of a single isoprene block, given by

$$v_{PI} = M_{PI}/(\rho_{PI} \times 0.602 \times 10^3) \tag{10}$$

With Eqs. (9) and (10), the volume fraction of homopolymer in the corona, $\Phi_{\text{homo,corona}}$ can be estimated from the following equation:

$$\Phi_{\text{homo,corona}} = 1 - \left[p v_{PS}/(4/3)\pi\left(R_{HS}^3 - R_c^3\right) \right] \tag{11}$$

where v_{PS} is the molecular volume of a single styrene block. Fig. 7 shows a plot of the volume fraction versus the ratio of molecular weight of PVME to that of styrene blocks, M_{PVME}/M_{StB}. The decreasing solubility of PVME in the micelle corona is due to the decreasing entropy from the mixing of PVME homopolymer and styrene block chains as the ratio, M_{PVME}/M_{StB} increases. For SI diblock copolymer and the PS mixture, Koizumi et al. have reported that macrophase separation occurs when the ratio of PS to styrene block molecular weight,

M_{PS}/M_{StB} is above 1 [22]. Therefore, one can see that in blends of SI/PVME having a ratio of M_{PVME}/M_{StB} above 1, the attractive interactions between styrene blocks of copolymer and PVME significantly induce the enthalpic driving force responsible for the solubility of PVME in the corona region.

Over the range of styrene block molecular weight studied, the increase in core radius can be described by the scaling behavior $R_c \propto M_{StB}^\alpha$ in Fig. 8(a). Here, α is found to be -0.30 ± 0.05, showing almost the same value for all concentrations studied within error of the measurements. This is lower than the value of $\alpha = -0.20$ determined from the data of Kinning et al. [9] for blends of SB diblock copolymer and low molecular weight PS ($M_{PS}/M_{StB} < 1$). It suggests that the solubility of PVME ($M_{PVME}/M_{StB} > 1$) into styrene blocks is higher than that of PS ($M_{PS}/M_{StB} < 1$) at room temperature. This phenomenon can also be found in the scaling of corona thickness described by $L \propto M_{StB}^\beta$. Fig. 8(b) shows a log–log plot of corona thickness versus styrene block molecular weight for SI4510, SI2510, and SI1510. Here, β is found to be 0.61 ± 0.05. A value of $\beta = 0.59$ would be expected for blends of SB diblock copolymer and low molecular weight PS [9]. A value of β greater than 0.59 also implies that a PVME of high molecular weight is more soluble than a PS of low molecular weight as found in the scaling behavior of the core radius. Even though the high molecular weight PVME has a disadvantage in terms of mixing entropy compared to the low molecular weight PS homopolymer, the attractive interaction between styrene block and PVME lead PVME chains to be more easily solubilized into styrene block by negative mixing enthalpy at room temperature
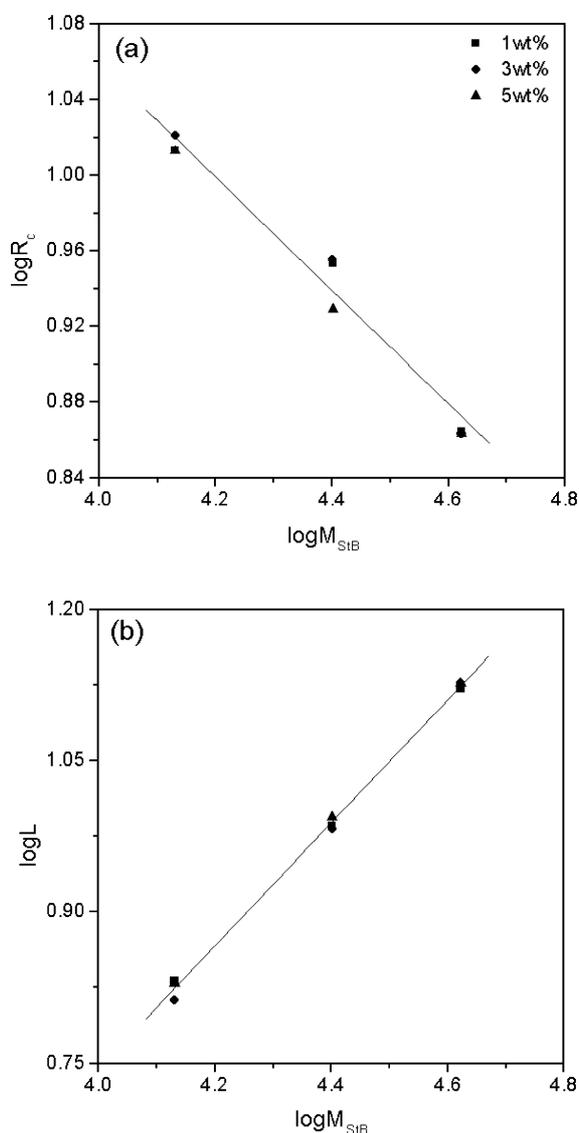
Fig. 8. (a) Core radius as a function of styrene block length for SI4510, SI2510, and SI1510. (b) Corona thickness as a function of styrene block length.

and by causing the styrene block chains to swell, overcoming the entropic disadvantage. Therefore, PVME has better solubility than PS homopolymer.

4. Conclusions

SAXS and TEM have been used to study the effect of styrene block length on the formation of micellar structure in blends of PVME and SI diblock copolymers. This study showed that the effect of styrene block length on micelle structure in PVME matrix is different from that in PS matrix. The scaling of micelle core size and corona thickness with styrene block length in PVME matrix has an absolute exponent value slightly greater than that in PS matrix. The scaling difference of the two blends arises from the change in homopolymer concentration in the micellar corona and related enthalpic effects. Such a scaling difference indicates that the solubilization of PVME ($M_{PVME}/M_{StB} > 1$) into the corona region (styrene block) is much greater than that of PS ($M_{PS}/M_{StB} < 1$) at room temperature. This led us to conclude that the attractive interactions between styrene blocks of copolymer and PVME significantly induce the enthalpic driving force responsible for the solubility of PVME in the corona region.

References

[1] Bates FS, Schulz MF, Khandpur AK, Förster S, Rosedale JH, Almdal K, Mortensen K. Faraday Discuss 1994;98:7.
[2] Zin WC, Roe RJ. Macromolecules 1984;17:183.
[3] Roe RJ, Zin WC. Macromolecules 1984;17:189.
[4] Winey KI, Thomas EL, Fetters LJ. Macromolecules 1992;25:422.
[5] Rigby D, Roe RJ. Macromolecules 1984;17:1778.
[6] Rigby D, Roe RJ. Macromolecules 1986;19:721.
[7] Roe RJ. Macromolecules 1986;19:728.
[8] Nojima S, Roe RJ, Rigby D, Han CC. Macromolecules 1990;23:4305.
[9] Kinning DJ, Thomas EL, Fetters LJ. J Chem Phys 1989;90:5806.
[10] Kinning DJ, Winey KI, Thomas EL. Macromolecules 1988;21:3502.
[11] Kinning DJ, Thomas EL. Macromolecules 1984;17:1712.
[12] Selb J, Marie P, Rameau A, Duplessix R, Gallot Y. Polym Bull 1983;10:444.
[13] Leibler L, Orland H, Wheeler JC. J Chem Phys 1983;79:3550.
[14] Whitmore MD, Noolandi J. Macromolecules 1985;18:657.
[15] Adedeji A, Hudson SD, Jamieson AM. Macromolecules 1996;29:2449.
[16] Iizuka N, Bodycomb J, Hasegawa H, Hashimoto T. Macromolecules 1998;31:7256.
[17] Ahn JH, Sohn BH, Zin WC, Noh ST. Macromolecules 2001;34:4459.
[18] Shimoi T, Hamada F, Nasako T, Yoneda K, Imai K, Nakajima A. Macromolecules 1990;23:229.
[19] Percus JK, Yevick GJ. Phys Rev 1958;110:1.
[20] Ashcroft NW, Lekner J. Phys Rev 1966;145:83.
[21] Kotlarchyk M, Chen SH. J Chem Phys 1983;79:2461.
[22] Koizumi S, Hasegawa H, Hashimoto T. Macromolecules 1994;27:6532.
[23] Ahn JH, Kang CK, Zin WC. Eur Polym J 1997;33:1113.
[24] Lee HK, Kang CK, Zin WC. Polymer 1997;38:1595.